

# PROCEEDINGS OF SPIE

[SPIDigitalLibrary.org/conference-proceedings-of-spie](https://SPIDigitalLibrary.org/conference-proceedings-of-spie)

## Curvature-based laser guide star adaptive optics system for Gemini South

Mark Richard Chun, Celine D'Orgeville, Brent L. Ellerbroek, J. Elon Graves, Malcolm J. Northcott, et al.

Mark Richard Chun, Celine D'Orgeville, Brent L. Ellerbroek, J. Elon Graves, Malcolm J. Northcott, Francois J. Rigaut, "Curvature-based laser guide star adaptive optics system for Gemini South," Proc. SPIE 4007, Adaptive Optical Systems Technology, (7 July 2000); doi: 10.1117/12.390399

**SPIE.**

Event: Astronomical Telescopes and Instrumentation, 2000, Munich, Germany

# A curvature-based laser guide star adaptive optics system for Gemini-South

Mark Chun<sup>a</sup>, Céline d'Orgeville<sup>a</sup>, Brent Ellerbroek<sup>a</sup>, J.E. Graves<sup>b</sup>, Malcolm Northcott<sup>b</sup>, François Rigaut<sup>a</sup>

<sup>a</sup>Gemini Observatory, 950 N. A'Ohoku Place, Hilo, HI 96720

<sup>b</sup>Institute for Astronomy, 2680 Woodlawn Drive, Honolulu, HI 96822

## ABSTRACT

The Gemini Observatory and University of Hawaii are planning to install an 85-element curvature adaptive optics system with a laser guide star system on its Cerro Pachón telescope in 2001. This paper discusses the motivation, issues on implementing a laser guide star with a curvature-based system, the implementation of a laser guide star based on a commercially available 2W ring-dye laser, and the expected performance of the system. Detailed simulations show very promising results for system performance down to natural guide star magnitudes of 19-20<sup>th</sup> magnitude. The performance cross-over point between NGS and LGS is between 13-16<sup>th</sup> magnitude depending on the performance parameter of interest (e.g. Strehl, energy through a slit, etc.)

**Keywords:** curvature sensing, laser guide star

## 1. INTRODUCTION

Observations with current adaptive optics systems are limited by the requirement of a bright near-by reference source. For astronomical adaptive optics systems (AOS) performance typically degrades for sources fainter than V~14. This limit depends strongly on the type of AOS as well as the intrinsic seeing at the site. However, an example of a system with one of the faintest limiting magnitudes is the University of Hawaii's Hokupaa on the Gemini-North telescope on Mauna Kea in Hawaii. While this system currently has only 36 correcting elements, it is at a good site and the wavefront sensor is a curvature sensor based on zero-read noise avalanche photo-diodes. Partial performance gains are seen with this system even at magnitudes as faint as magnitude R~17. However even this system is limited in sky coverage.

To address the issue of sky coverage several groups have begun implementing artificial guide stars using a tuned laser to excite a resonance line of sodium atoms in the mesosphere<sup>1,2,3</sup>. All orders spatially higher than tip and tilt are corrected using the wavefront measured from this artificial source. A natural guide star is required for measuring the tip and tilt but since the entire telescope aperture can be used for this, the limiting magnitude of the required natural guide star is fainter. In addition, since the isoplanatic angle for the tip and tilt modes is larger than the higher order modes, the sky coverage is larger. Moreover, for spectroscopic applications, the slit throughput degrades slowly for increasing tip/tilt variance for slits larger than the diffraction limit.

In practice the implementation of a sodium laser guide star has been difficult<sup>1,2</sup>. Implementing the LGS with a curvature-based system brings two key advantages to ease the process. First, the curvature-based adaptive optics system has already proven itself to be robust and reliable. In particular, the system is less sensitive to optical misalignment than a Shack-Hartmann-based system. Second, because the wavefront sensor is based on zero read-noise APDs, the LGS brightness requirement is greatly relaxed compared to CCD-based AOS. This fact lowers the required photon return rate to below a critical threshold to allow the use of commercial, off-the-shelf laser components running at the manufacturer's nominal power levels.

In this paper we discuss the issues in implementing a LGS with a curvature-based system, describe the modifications to the natural guide star AOS, discuss the components of the LGS, and finally present the expected performance of the system within the context of the focal-plane instrumentation and science observations.

## 2. MOTIVATION

We expect that the gains from adding a LGS to a curvature-based AOS will be substantial. Expected gains over the NGS mode are (1) high-order corrections are independent of the NGS magnitude, (2) sensing of the higher-order aberrations on-axis negates higher-order angular anisoplanatism errors, and (3) an optimized sensor can be used to sense the tip/tilt errors from the NGS. These advantages should lead to an increase in the sky coverage of the adaptive optics system. The use of a LGS to sense the wavefront aberration modes higher than tip and tilt fixes the level of wavefront correction for these modes. Namely, the photon noise and bandwidth errors in the wavefront correction are small if the LGS is sufficiently bright. In addition, because the LGS is placed on- or very nearly on-axis with the science object, the angular anisoplanatism error for the higher-order terms is negligible. There is a trade in performance between using an AOS with a NGS off-axis and using an AOS with a LGS 'on-axis' since the LGS wavefront includes errors due to focal-anisoplanatism. From the results of the Cerro Pachon site survey<sup>4</sup>, the mean isoplanatic angle in the visible is 2.6 arcseconds while the mean scale length for focal-anisoplanatism ( $d_0$ ) is 3.8 meters. Scaling both of these quantities into the H-band (1.65 microns) give characteristic errors in which the angular anisoplanatism error is larger than the focal-anisoplanatism error for NGS further than  $\sim 5$  arcseconds from the source of interest.

$$(\theta/\theta_0)^{5/3} > (D/d_0)^{5/3}$$

This is an over-simplification of the actual performance trades since the isoplanatic error is over estimated by  $(\theta/\theta_0)^{5/3}$  and a significant portion of this error is due to the tilt anisoplanatism which the LGS system still incurs. However, it illustrates the point that there is an advantage to sensing the higher-order aberrations on-axis with the laser guide star to using a natural guide star off-axis.

By decoupling the higher-order modes from the tip and tilt, we can now optimize the NGS sensor for the required lowest order modes. Consider a curvature sensor sensing all wavefront modes. For a given photon flux and seeing condition, the optical gain (extrafocal distance in the measurement) must be balanced with the order of the correction. For sensing higher order modes, larger extra-focal distances are needed. However, it is evident from the relationship between the measured irradiance patterns ( $I_1, I_2$ ) and the wavefront ( $\varphi$  and  $\partial\varphi/\partial n$ ) that increasing the extra-focal distance however decreases the sensitivity of the sensor since the measured signal decreases with increasing optical gain ( $\ell$ ) for a given wavefront aberration<sup>5</sup>.

$$\frac{I_1 - I_2}{I_1 + I_2} = \frac{\lambda f (f - \ell)}{2\pi\ell} \left[ \frac{\partial\varphi}{\partial n} \left( \frac{f\mathbf{r}}{\ell} \right) \delta_c - \nabla^2 \varphi \left( \frac{f\mathbf{r}}{\ell} \right) \right]$$

This means that for the tip & tilt modes the optimal extra-focal distance is small. As pointed out by Rousset (1994), in this limit the curvature sensor becomes a quad-cell that uses the entire aperture for sensing wavefront tip/tilt errors. In the case of an LGS AOS, the NGS is used only for tip and tilt however it may be convenient to sense focus as well due to the varying distance to the sodium layer so we plan to implement either a quad-cell or a low-order curvature sensor.

Finally we note that while the atmospheric tip and tilt phase variances are the largest, the effect of residual tip/tilt errors is simply image smear. In the focal-plane of a slit or integral-field spectrograph, if the higher-order aberrations are well corrected (i.e. there is a diffraction-limited core in the short-exposure PSF), then the degradation in slit throughput is small.

## 3. AO AND LGS CONFIGURATION

The details of the NGS 85-element adaptive optics system can be found in Graves et al.<sup>6</sup> The basic modification to the AOS to accommodate a laser guide is the addition of a steerable NGS acquisition mirror, a NGS tip/tilt quad-cell sensor, and a stage to accommodate the variable range to the LGS.

The overall Cerro Pachón LGS system consists of five major subsystems: Laser System, Beam Transfer Optics, Laser Launch Telescope, LGS Control System, and Safety Systems. The CP LGS system will be implemented and integrated on the telescope in 2001. The LGS system will be based around a 2W continuous-wave single-mode laser. The power requirement was derived from the performance analysis of and detailed calculations of the interaction of photons with the

sodium atoms in the mesosphere by Telle et al.<sup>7</sup>. The requirement accounts for the beam transfer efficiency along the upward and downward paths, as well as the detailed physics of the interaction at the sodium layer of a single-mode CW laser<sup>8</sup>. Under the assumption of a low sodium column density and an optical efficiency in the beam propagation from the laser to the sodium layer of 40%, the 2W requirement translates into a photon flux of 37.4 photons sec<sup>-1</sup> cm<sup>-2</sup>. This number was derived for a median-to-low sodium column density of 2 x 10<sup>9</sup> cm<sup>2</sup>, 30 degrees from the zenith, and an optical efficiency from the laser to the mesosphere of 43%. The photon flux translates into a LGS magnitude of about V~11.0 at the ground.

A number of commercial lasers can produce the specified 2 Watts at good beam quality at the sodium D2 line. A ring dye laser, similar to the lasers used by the Max Planck Institute für Astronomie and the University of Arizona have reached power levels as high as 4 Watts when pumped by a 25 W Argon-ion laser. In our case, the reduced power requirements allow a simplification to be made with regard to the pump laser. Our pump laser will be a continuous-wave 10 W doubled Nd:YVO4 laser @ 532 nm. There are two possible suppliers for this diode-pumped solid-state laser: the Verdi by Coherent and the Millennia X by Spectra Physics. Both companies have demonstrated 2.5 W of single frequency operation out of a solid-state pumped dye laser emitting at 589 nm and will warranty our 2 W output power requirement over 5000 hours of operation (about 500 nights of LGS operation). We will need to make some modifications to the laser system to turn it into an efficient, fully automated source. These include a sodium cell to lock the laser frequency on the peak of the sodium D2 line, modifying the laser frequency control loop electronics, and replacing the dye nozzle and the dye pump with high pressure systems.

The dye laser cannot be located on the telescope itself because the use of an open-air dye jet requires mounting the laser horizontally and monomode lasers are very sensitive to vibrations, temperature variations and dust. Instead, the laser will be mounted in a stable environment, possibly in a room under the cable-wrap in the telescope pier. It will be mounted on an isolated table, in a thermally controlled enclosure. We will also use filtered air above the laser optics in order to prevent dust deposit.

The beam transfer optics brings the laser output beam to the launch telescope on the top-end of the Gemini telescope. The positioning of the LGS on the sky is controlled by this subsystem. The system includes active control of the beam direction and supply diagnostics on the beam pointing (far- and near-field), an indication of the beam quality, and the beam power. The nominal design consists of a train of about 15 high quality, high reflectivity dielectric mirrors optimized for 589 nm, a relay telescope to control the beam size on the laser launch telescope, a slow steering mirror for dithering, and a fast steering mirror to stabilize the LGS in the WFS. At these power levels scattering from aerosols or smaller particles does not increase the background in the WFS detector. However, in anticipation of future higher-power LGS projects at Gemini-South, the beam path may be enclosed along the telescope structure.

On the top-end, behind the secondary, we will place a beam-expanding telescope. Two main configurations are available for designing the laser launch telescope (LLT): it could be off-axis attached to the side of the main telescope, or on-axis mounted behind the secondary mirror. Gemini has chosen the on-axis configuration. While this requires a more careful implementation, it minimizes the laser power and facilitates the LGS wavefront sensing. Our current design is equivalent to a Keplerian beam expander with a deployable primary mirror to ensure that the infrared background of the Gemini telescope is not increased when the LGS is not in use. To simplify the integration of the system, the LLT is envisioned as a stand-alone instrument mounted in its own structure with specific interfaces to the secondary frame. This allows the unit to be tested and aligned before mounting on the telescope.

#### 4. EXPECTED PERFORMANCE

To determine the level of performance with such a system, Monte-Carlo simulations were run using a package developed by F. Rigaut. This package includes :

- (1) multiple layered phase screen turbulence,
- (2) temporal evolution of the turbulence assuming "frozen" turbulence,
- (3) full simulation of the image formation in the curvature sensor including focal-anisoplanatism,
- (4) deformable mirror influence functions, and
- (5) laser projection including propagation through the atmosphere and spot elongation.

Simulations were made for both the LGS and NGS configuration. In each case (NGS and LGS), we first optimized the extra-focal distance. For the LGS case this was optimized for a 12th magnitude LGS. The difference between the above LGS magnitude of 11.0 and 12.0 takes into account the expected transmission losses from the telescope to the wavefront sensor detectors. In the case of the LGS AOS we next optimized the higher-order control servo. Simulation runs on the NGS magnitude (tip/tilt only for the LGS case) were then made. The parameters used in the simulations are summarized in the table below.

**Table 1 Summary of simulation parameters**

<b>Telescope</b>	diameter	7.9 m	
	central obscuration	0.1295	
<b>Atmosphere</b>	$D/r_0$ (@ $\lambda_{LGS}$ )	43.8	
	$r_0$ (0.5 $\mu$ )	16.6 cm	
	$\theta_0$ (0.5 $\mu$ )	2.6 arcsec	
	$C_N^2$ distribution		
		<i>altitude (km)</i>	<i><math>V_{wind}</math> (m/s)</i>
	2.7	6.7	0.64
	4.5	8.3	0.08
	6.0	13.4	0.119
	8.5	25.6	0.035
	10.1	33.9	0.025
	15.75	22.2	0.08
	18.5	8.9	0.015
<b>Sensor</b>	$\lambda_{WFS}$	589 nm	
	extra-focal distance	0.7 m	
	field size	4.0 arcsec	
<b>Laser guide star</b>	sodium layer altitude	95 km	
	sodium layer thickness	8 km	
	launch telescope location	<i>behind telescope secondary</i>	
	beam waist diameter	0.3 m	
	launch telescope diameter	0.45 m	
	LGS magnitude	12.0	
		<i>(corresponding to 11.0 at entrance of telescope)</i>	
	off-axis angle	0.0 (LGS-mode) 0.0 (NGS-mode)	
sky magnitude	20.7 mag / arcsec <sup>2</sup>		
<b>NGS tip/tilt guide star</b>	magnitude	13 – 21	
	sky magnitude	19.2 magnitude / arcsec <sup>2</sup>	
	pixel size	0.5 arcsec/APD	
	field of view	2x2 APDs	
	$\lambda_{TT}$	700 nm	
	offaxis angle	30.0 arcsec	

The H-band (1.65 micron) performance of the AOS in NGS and LGS mode is given in Figure 1 below. Note that these performance estimates are for the adaptive optics system only so telescope and instrument errors must still be considered. Also note that for both the NGS and LGS cases the guide star is assumed to be on-axis. The anticipated cross-over in performance between the NGS and LGS modes is evident and occurs around R-13 in the Strehl. Figure 1 also shows the expected slit throughput for slit widths of 1.5x and 2.5x the diffraction-limited width for a point source. This figure and the

figure for the 50% encircled energy diameter illustrate that increasing residual tilt errors maintain the observation sensitivity limit out to magnitudes of 18-19. At this point, the sky background becomes the limiting noise source in the tip/tilt sensor and the sensitivity drops rapidly. Although not shown, simulations at other wavelengths were also run. Good performance is given for wavelengths greater than 1 micron. For example, the LGS AOS system at a NGS (tip/tilt only) magnitude of R~17 gives a Strehl at 1 micron of only 5% but a FWHM of about two times the diffraction limit (~55mas).

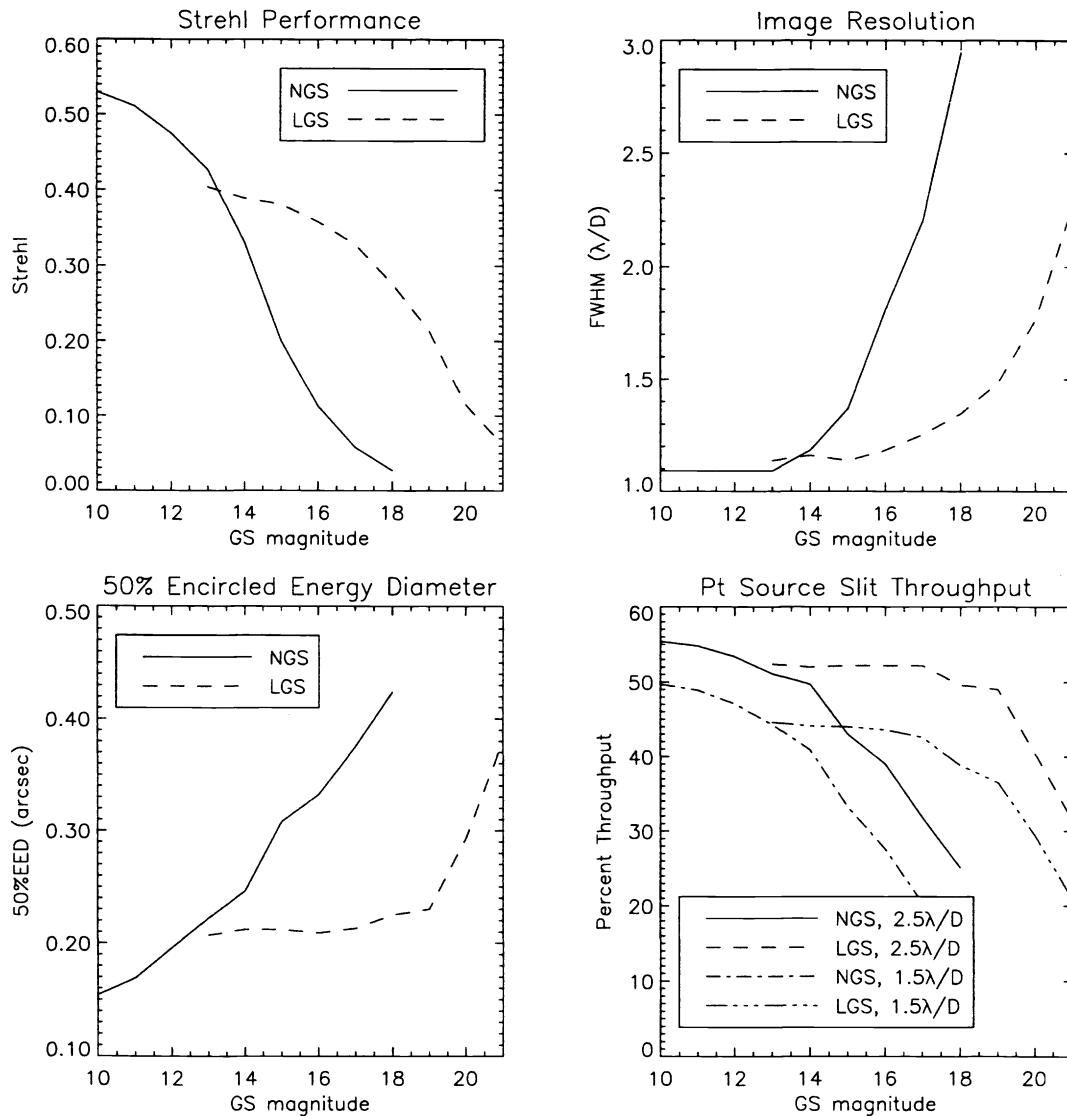


**Figure 1 Estimated system performance (AOS only)**

Taking the star counts of Bahcall and Soneira<sup>9</sup> we find that at the  $R \leq 18$ th magnitude there are roughly 3000 (galactic latitude=30 degrees) and 1000 (galactic pole) stars per square degree. For an NGS patrol field radius of 30 arcseconds this translates into a sky coverage of between 20-50% depending on the galactic latitude. Importantly, as illustrated in Figure 2, slit throughput above 30% can be obtained for most of the sky. In this figure, the tip/tilt guide star is assumed to be 30" from the science target. The advantage of the NGS-mode is limited to the lower righthand corner of the plot where the throughput is the highest but the sky coverage is very low.

**Table 2. Sky Coverage past for fainter limiting magnitudes**

NGS magnitude	15	16	17	18	19	20
galactic latitude = 30	12%	23	35	48	73	76
galactic latitude = 90	4%	8	12	20	28	35

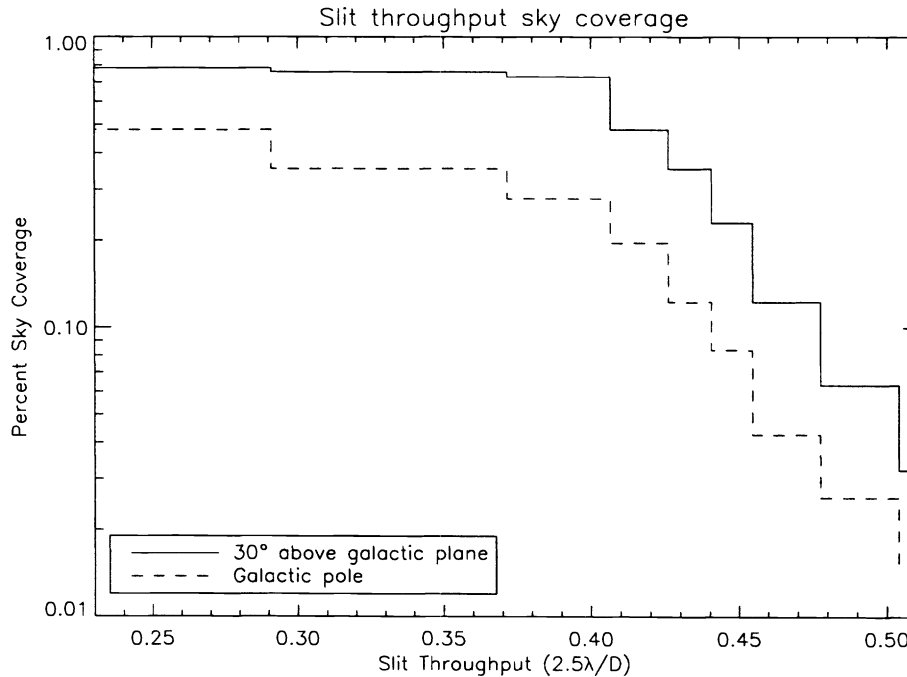


**Figure 2. Sky coverage as a function of slit throughput**

At these limiting magnitudes, we can begin to consider other astrophysical objects as viable tracking sources. For example, galactic cores or bright star formation regions are often compact and brighter than  $R\sim 19-20$ . As an example we note that the distribution of quasar brightnesses peaks around  $v\sim 18$ . From this target set, systematic studies of the fields around quasars can be made out to redshifts of  $z\sim 4$ .

## 5. CONCLUSIONS

A curvature-based adaptive optics system outfitted with a laser guide star on the Gemini-South telescope is expected to give good performance in image resolution and slit throughput for a significant fraction of the sky. The LGS system extends the image correction capabilities to limiting NGS magnitudes of  $R\sim 19$ . At this limit more than one third of the sky is observable. The use of avalanche photo diodes allows the use of a lower-cost commercial laser to pump the mesospheric sodium layer. We expect that from a 2-Watt laser we will have sufficient photon return to use the system in all conditions.

## 6. REFERENCES

1. S. Olivier et al. 1999, "Improved performance of the laser guide star adaptive optics system at Lick Observatory", Proc. SPIE Vol 3762 p. 2-7.
2. S. Hippler et al. 1998, "ALFA: the MPIA/MPE adaptive optics with a laser project", Proc. SPIE Vol 3352, 44-55.
3. E. Kibblewhite and F Shi, "Design and field-tests of an 8-W sum-frequency laser for adaptive optics", Proc SPIE Vol 3353, 300-309.,1998

4. R. Avila et al , "Turbulence and Wind Profiling with Generalized SCIDAR at Cerro Pachon", these proceedings, 2000
5. G. Rousset, G., in Adaptive Optics for Astronomy Ed. D.M. Alloin and J.-M. Mariotti., 1994
6. J.E. Graves et al., these proceedings, 2000.
7. John M. Telle, Peter W. Milonni, and Paul D. Hillman, "Comparison of pump-laser characteristics for producing a mesospheric sodium guidestar for adaptive optical systems on large-aperture telescopes", SPIE Proceedings vol. 3264, 1998
8. C. d'Orgeville et al., "Gemini Mauna Kea Laser Guide Star system", SPIE Proceedings vol. 3762, 1999.
9. Bahcall and Soneira 1984, ApJS, 55, 67.